

# Removal of SO<sub>2</sub> and the Simultaneous Removal of SO<sub>2</sub> and NO from Simulated Flue Gas Streams Using Dielectric Barrier Discharge Plasmas

Moo Been Chang,<sup>1,3</sup> Mark J. Kushner,<sup>2</sup> and Mark J. Rood<sup>1,4</sup>

Received January 16, 1992; revised March 13, 1992

---

*A gas-phase oxidation method using dielectric barrier discharges (DBDs) has been developed to remove SO<sub>2</sub> and to simultaneously remove SO<sub>2</sub> and NO from gas streams that are similar to gas streams generated by the combustion of fossil fuels. SO<sub>2</sub> and NO removal efficiencies are evaluated as a function of applied voltage, temperature, and concentrations of SO<sub>2</sub>, NO, H<sub>2</sub>O<sub>(g)</sub>, and NH<sub>3</sub>. With constant H<sub>2</sub>O<sub>(g)</sub> concentration, both SO<sub>2</sub> and NO removal efficiencies increase with increasing temperature from 100 to 160°C. At 160°C with 15% by volume H<sub>2</sub>O<sub>(g)</sub>, more than 95% of the NO and 32% of the SO<sub>2</sub> are simultaneously removed from the gas stream. Injection of NH<sub>3</sub> into the gas stream caused an increase in SO<sub>2</sub> removal efficiency to essentially 100%. These results indicate that DBD plasmas have the potential to simultaneously remove SO<sub>2</sub> and NO from gas streams generated by large-scale fossil fuel combustors.*

---

**KEY WORDS:** Dielectric barrier discharge; SO<sub>2</sub> removal; NO removal; gas-phase oxidation.

## 1. INTRODUCTION

SO<sub>2</sub> and NO<sub>x</sub> (including NO and NO<sub>2</sub>) have been known to be gaseous air contaminants for decades. They have adverse effects on human health,<sup>(1)</sup> damage vegetation,<sup>(2)</sup> and degrade materials.<sup>(3)</sup> SO<sub>2</sub> and NO are also the

<sup>1</sup>Department of Civil Engineering, University of Illinois, 205 N. Mathews Avenue, Urbana, Illinois 61801-4723.

<sup>2</sup>Department of Electrical and Computer Engineering, University of Illinois, 1406 W. Green Street, Urbana, Illinois 61801-4723.

<sup>3</sup>Present address: Graduate Institute of Environmental Engineering, National Central University, Chungli, Taiwan 32054.

<sup>4</sup>To whom correspondence should be sent.

two most important gaseous air contaminants that contribute to acid rain which has had detrimental effects on ecosystems in North America and Europe.<sup>(4)</sup> In addition,  $\text{SO}_2$  and  $\text{NO}$  contribute to the degradation of visibility since they form accumulation-mode aerosol particles containing sulfates and nitrates.<sup>(5,6)</sup> Furthermore,  $\text{NO}$  chemically reacts with gaseous hydrocarbons in the atmosphere to form noxious photochemical contaminants such as  $\text{O}_3$  and peroxyacetyl nitrate (PAN).<sup>(7)</sup> In recent years, the degradation of visibility at some national parks in the United States and the widespread failure to satisfy the National Ambient Air Quality Standards for  $\text{O}_3$  in large metropolitan areas such as Los Angeles and Chicago have caused public concern.<sup>(8,9)</sup>

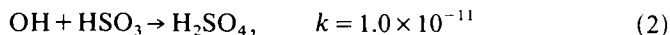
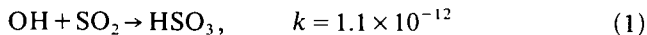
As the emission standards for  $\text{SO}_2$  and  $\text{NO}_x$  become more stringent as described in the 1990 Clean Air Act Amendments, the cost to achieve these standards also escalates. Given the constraints of current technology for removing  $\text{SO}_2$  and  $\text{NO}$  from gas streams, it would be useful to simultaneously remove  $\text{SO}_2$  and  $\text{NO}$  from gas streams in a single process that is not as complicated or expensive as existing technology. Gas-phase oxidation processes using electron beams (e-beams) have been demonstrated as an effective technology to simultaneously remove  $\text{SO}_2$  and  $\text{NO}$  from gas streams.<sup>(10-12)</sup> With  $\text{NH}_3$  injection, removal efficiencies for  $\text{SO}_2$  ( $\eta_{\text{SO}_2}$ ) and  $\text{NO}$  ( $\eta_{\text{NO}}$ ) were over 90 and 80%, respectively.<sup>(13)</sup> Nevertheless, the high cost and potential X-ray hazard of the process have motivated research to develop more effective gas-phase oxidation processes.

This paper discusses dielectric barrier discharge (DBD) plasmas, also known as silent discharges, as an innovative gas-phase oxidation process that simultaneously removes  $\text{SO}_2$  and  $\text{NO}$  from gas streams. This process uses DBDs to generate gas phase radicals, such as hydroxyl (OH), hydroperoxyl ( $\text{HO}_2$ ), and oxygen atom (O), that simultaneously oxidize  $\text{SO}_2$  and  $\text{NO}$  to form particles consisting of  $\text{H}_2\text{SO}_4$  and  $\text{HNO}_3$ , respectively. The particles can then be chemically neutralized with  $\text{NH}_3$  to form  $(\text{NH}_4)_2\text{SO}_4$  and  $\text{NH}_4\text{NO}_3$ . In an industrial application of this process, the particles could then be removed from the gas stream by a particle removal device, such as a fabric filter or electrostatic precipitator.<sup>(14)</sup> A DBD was chosen for this study because of its relatively low cost and high efficiency at generating gas-phase radicals.<sup>(15)</sup>

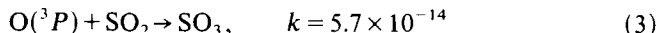
## 2. GAS-PHASE REMOVAL MECHANISMS

The goal of treating  $\text{SO}_2$  and  $\text{NO}$  contaminated gas streams is their conversion to  $\text{H}_2\text{SO}_4$  and  $\text{HNO}_3$  since these compounds are more easily removed from the gas stream. Gas-phase oxidation of  $\text{SO}_2$  by OH produces  $\text{HSO}_3$  and  $\text{H}_2\text{SO}_4$  as shown in Reactions (1) and (2).<sup>(16,17)</sup> (The reaction

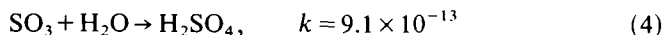
rate constants denoted by  $k$  listed below are evaluated at 25°C. They have units cm<sup>3</sup> s<sup>-1</sup> unless otherwise noted.)



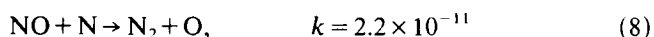
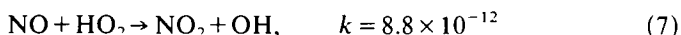
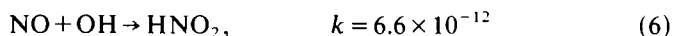
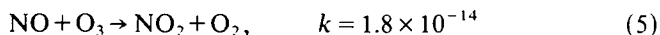
O(<sup>3</sup>P) generated in a plasma can also oxidize SO<sub>2</sub> to form SO<sub>3</sub>.<sup>(16)</sup>



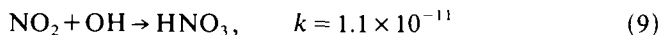
SO<sub>3</sub> is hygroscopic and can be hydrolyzed to form H<sub>2</sub>SO<sub>4</sub> if H<sub>2</sub>O is available.<sup>(16)</sup>



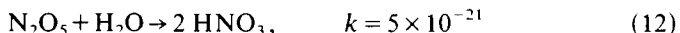
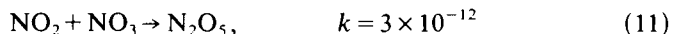
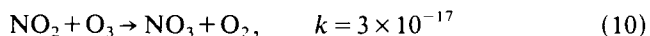
NO can rapidly react with O<sub>3</sub> and is a more efficient free radical scavenger than SO<sub>2</sub>. The reactions believed to process NO are presented below.<sup>(18-20)</sup>



NO<sub>2</sub> is also oxidized by OH radicals to form the desired product HNO<sub>3</sub>.<sup>(19)</sup>



NO<sub>2</sub> can also be oxidized to NO<sub>3</sub> by O<sub>3</sub>. NO<sub>3</sub> can then react with NO<sub>2</sub> to form N<sub>2</sub>O<sub>5</sub>. N<sub>2</sub>O<sub>5</sub> can then be hydrolyzed to form HNO<sub>3</sub>.<sup>(21)</sup>



Based on this discussion of reactions of SO<sub>2</sub> and NO, to form H<sub>2</sub>SO<sub>4</sub> and HNO<sub>3</sub>, and in the context of industrial treatment of large volumetric flow rates, it is essential that gas-phase radicals, such as OH, HO<sub>2</sub>, and O, be generated efficiently. There are many plasma-based radical generation techniques, but it is not clear that they are either efficient or scalable.

### 3. DIELECTRIC BARRIER DISCHARGE PROCESS

DBDs have been widely used as O<sub>3</sub> generators with industrially acceptable efficiencies.<sup>(22)</sup> In DBDs a dielectric material is placed on one of the two discharge electrodes.<sup>(23)</sup> Typically, the insulating material has a high

dielectric strength and a high dielectric constant (e.g., glass or ceramic). When the electrical potential across the discharge gap reaches the breakdown voltage, the dielectric acts as a stabilizing material leading to the formation of a large array of microdischarges of short pulses which are distributed spatially and temporally over the discharge gap.<sup>(23)</sup> Typical duration of these microdischarges is of the order of nanoseconds to some hundreds of nanoseconds depending on the gas composition and discharge configuration.<sup>(15)</sup> The typical electron temperatures in the microdischarges are a few to 10 eV. These plasmas are ideal for generation of gas-phase radicals in atmospheric-pressure systems.

DBDs have been studied by other researchers to remove  $\text{SO}_2$ <sup>(24-26)</sup> and organic compounds such as benzene ( $\text{C}_6\text{H}_6$ ) and trichloroethylene ( $\text{C}_2\text{HCl}_3$ )<sup>(27-29)</sup> from gas streams. Sardja and Dhali<sup>(25)</sup> reported values of  $\eta_{\text{SO}_2}$  of about 50% with an applied voltage of 24 kV ac (peak to peak) and an inlet  $\text{SO}_2$  concentration ( $[\text{SO}_2]$ ) between 1000 and 5000 ppmv in a dry gas stream containing  $\text{N}_2$  and  $\text{O}_2$ . They proposed that oxidation of  $\text{SO}_2$  occurred by reaction with O radical to form  $\text{SO}_3$ . Research with e-beams indicated that in a dry gas stream, the resulting  $\text{SO}_3$  would react with O radical to form  $\text{SO}_2$  and  $\text{O}_2$ .<sup>(12)</sup> Sardja and Dhali's<sup>(25)</sup> results thereby imply either total utilization of any O radicals by  $\text{SO}_2$  or rapid surface or gas-phase recombination of the O atoms. Experimental results obtained at room temperature by Chang *et al.*<sup>(26)</sup> are consistent with results by Tokunaga *et al.*,<sup>(12)</sup> indicating that  $\text{H}_2\text{O}_{(g)}$  is necessary for  $\text{SO}_2$  removal with plasmas.

#### 4. EXPERIMENTAL DESIGN

The experimental apparatus consists of a continuous-flow gas generation system, laboratory-scale DBD reactor, and gas detection system (Fig. 1). The system was described in detail by Chang *et al.*,<sup>(30)</sup> but is briefly described for clarity.

Gas streams containing  $\text{N}_2$ ,  $\text{O}_2$ , and  $\text{CO}_2$  were initially heated to about 350°C to ensure complete evaporation of  $\text{H}_2\text{O}_{(l)}$  droplets that were injected into the gas stream with a peristaltic pump downstream of the heater.  $[\text{H}_2\text{O}_{(g)}]$  of the gas stream was controlled by regulating the volume feed rate of  $\text{H}_2\text{O}_{(l)}$  injected into the gas stream.  $\text{SO}_2$  and NO were then added to generate gas streams with known gas compositions, temperatures, and mass flow rates. These gas streams simulated the composition and temperature of gases that result from the combustion of fossil fuels. The gas stream was maintained at atmospheric pressure for all tests.

The DBD reactor was made of a quartz tube with 4 cm inner diameter and 0.2 cm wall thickness. The reactor's inside diameter of 4 cm is large

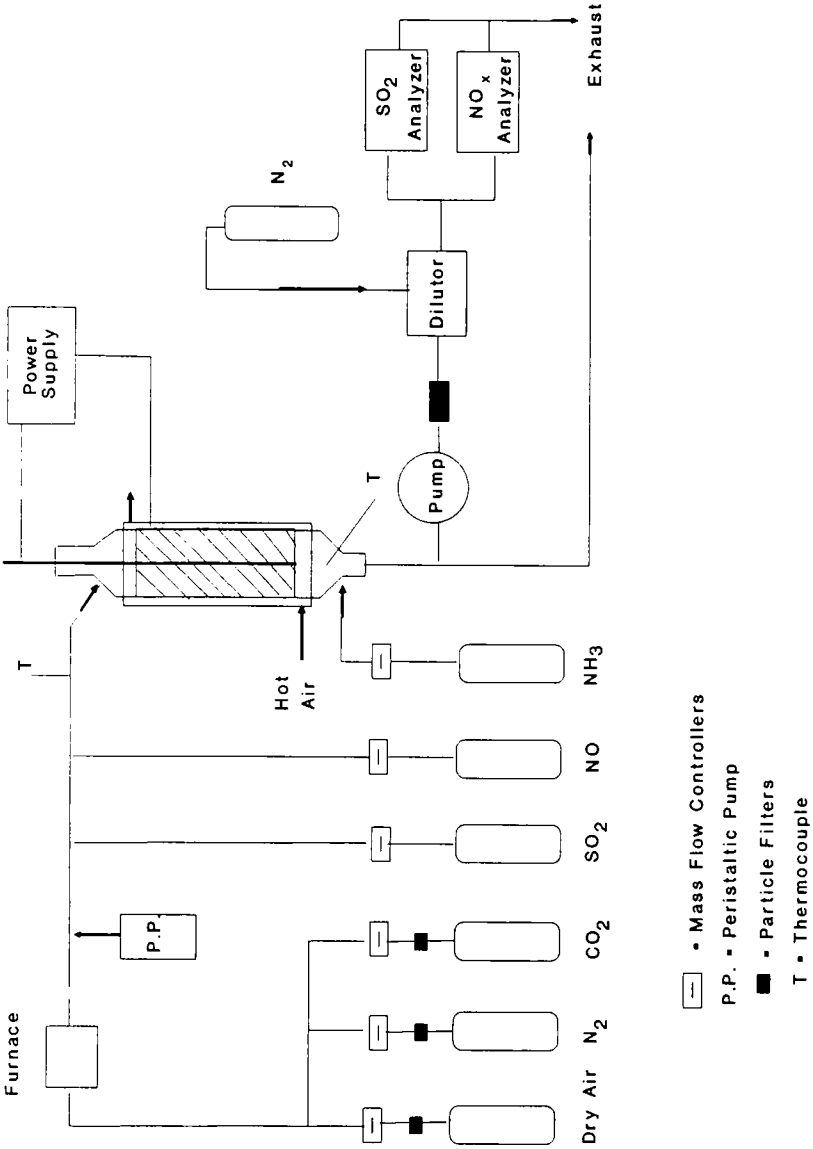


Fig. 1. Schematic of the gas generation system, dielectric barrier reactor, and gas sampling and detection system.

compared to the inside diameters used in DBD reactors for  $O_3$  generation. The larger gap spacing was used to minimize the pressure drop across the cell at high gas flow rates, as would be necessary in industrial applications of this process. One of the coaxial electrodes was made of a 0.24-cm-diameter tungsten rod and the other was stainless steel wire mesh. The rod and wire mesh electrodes were located vertically along the centerline and wrapped around the outside of the reactor, respectively. A 4-mm-diameter glass ball covered the end of the inner electrode to inhibit formation of corona. Near isothermal conditions ( $\pm 5^\circ\text{C}$ ) within the reactor were achieved by forcing countercurrent hot air through a concentric quartz tube surrounding the DBD reactor. The plasma volume was about  $350\text{ cm}^3$ . The discharge was sustained by a variable voltage transformer operating at 60 Hz. Depending on the temperature and composition of the gas stream, visible discharges were generally observed with voltage settings larger than 21 kV ac (peak value).

$[\text{SO}_2]$  and  $[\text{NO}]$  were monitored with a fluorescence-detection analyzer and a chemiluminescence-detection analyzer, respectively, after dilution with dry-grade  $\text{N}_2$ . Dilution was necessary to cool and reduce  $[\text{H}_2\text{O}_{(g)}]$ ,  $[\text{SO}_2]$ , and  $[\text{NO}]$  in the gas stream before detection. Prior to the experiments, each analyzer was calibrated with gas streams containing known mixtures of  $\text{SO}_2$  and  $\text{NO}$  to ensure that interferences with the detection of  $\text{SO}_2$  and  $\text{NO}$  did not occur when both gases co-existed in the gas stream.

The  $\text{NO}_x$  detector (Monitor Lab. Model 8840) is a gas-phase technique that detects the chemiluminescence of activated  $\text{NO}_2$  species ( $\text{NO}_2^*$ ) that are generated by the reaction of  $\text{NO}$  with  $\text{O}_3$ . The device is able to determine concentrations of  $\text{NO}$  and  $\text{NO}_x$  (the sum of  $[\text{NO}]$  and  $[\text{NO}_2]$  assuming the lack of any significant interferences) by selectively treating the sample stream with  $\text{O}_3$  or with a catalytic converter and  $\text{O}_3$ . The catalytic converter is used to chemically reduce  $\text{NO}_x$  to  $\text{NO}$  before  $\text{NO}$  reacts with  $\text{O}_3$ . Evaluation of the chemiluminescence detection of  $\text{NO}$  and  $\text{NO}_x$  has indicated that other oxides of nitrogen (besides  $\text{NO}$  and  $\text{NO}_2$ ) are detected by the  $\text{NO}_x$  analyzer.<sup>(31)</sup> All tests performed with the DBD reactor included measurements of  $\text{NO}_x$  and  $\text{NO}$  as discussed in Section 5. A more general detector for  $\text{NO}_x$  in the gas stream, such as a gas chromatograph-mass spectrometer, was not available for these experiments.

Initial conditions were recorded after the system reached steady-state conditions with no power applied to the reactor. Voltage from the power supply was then increased up to 25 kV (peak value) to generate DBDs.  $[\text{SO}_2]$  and  $[\text{NO}]$  were then recorded when their new values stabilized. The power supply was then shut off and the system was monitored to ensure that the system returned to its initial condition.  $\eta_{\text{SO}_2}$  and  $\eta_{\text{NO}}$  were then determined by the difference between their initial concentrations and their

stabilized concentrations divided by their initial concentrations. For instance,  $\eta_{\text{NO}}$  was determined by

$$\eta_{\text{NO}}(\%) = \left( \frac{[\text{NO}_{\text{off}}] - [\text{NO}_{\text{on}}]}{[\text{NO}_{\text{off}}]} \right) (100\%) \quad (13)$$

where the subscripts denote if the power supply for the DBDs was on or off.

## 5. RESULTS AND DISCUSSION

The dependences of  $\eta_{\text{SO}_2}$  on  $[\text{H}_2\text{O}_{(\text{g})}]$  of the gas stream at 100, 130, and 160°C were initially investigated at 25 kV (peak value) (Fig. 2). The gas flow rate was 2.7 slpm which corresponds to a gas residence time of 5.3 s in the discharge volume for a gas stream at 130°C and 1 atm. Inlet  $[\text{SO}_2]$  was 1000 ppmv,  $[\text{CO}_2]$  and  $[\text{O}_2]$  were 12 and 6% by volume, respectively, and  $\text{N}_2$  was the carrier gas. These conditions are typical for gas streams passing through air pollution control devices used downstream of fossil fuel combustors. For dry conditions ( $[\text{H}_2\text{O}_{(\text{g})}] \leq 3$  ppmv),  $\eta_{\text{SO}_2}$  was low ( $\leq 7\%$ ) due to the lack of OH radicals.<sup>(26)</sup> These operating conditions were chosen to determine how  $[\text{H}_2\text{O}_{(\text{g})}]$  would affect  $\eta_{\text{SO}_2}$  and to compare our results with those reported by Sardja and Dhali.<sup>(25)</sup> As  $[\text{H}_2\text{O}_{(\text{g})}]$  increased from 0 to 15% by volume,  $\eta_{\text{SO}_2}$  increases monotonically from 7 to 36% at

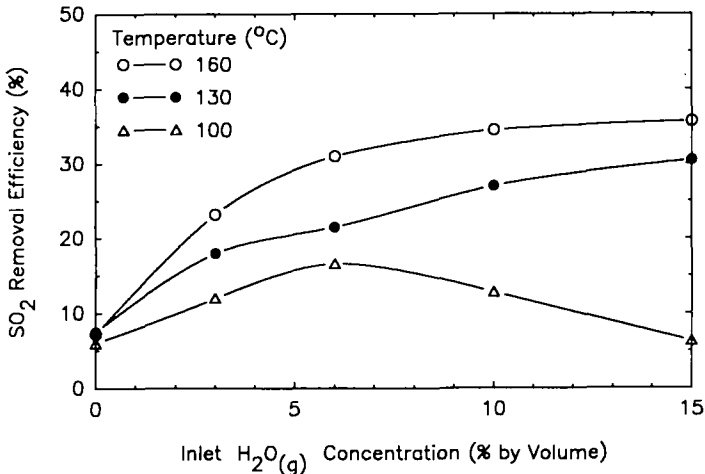


**Fig. 2.** Dependence of  $\eta_{\text{SO}_2}$  on inlet  $[\text{H}_2\text{O}_{(\text{g})}]$  at specified dry-bulb temperatures and 25 kV. Gas streams contain  $\text{SO}_2/\text{O}_2/\text{CO}_2 = 0.1\%/6\%/12\%$  by volume, and  $\text{N}_2$  as the carrier gas. Increasing  $[\text{H}_2\text{O}_{(\text{g})}] > 6\%$  by volume can either increase or decrease  $\eta_{\text{SO}_2}$  depending on the minimum required  $E/N$  value.

160°C.  $\eta_{\text{SO}_2}$  changes in the same manner at 130°C, whereas at 100°C,  $\eta_{\text{SO}_2}$  reaches a local maximum value at 6% by volume  $\text{H}_2\text{O}_{(\text{g})}$  and then decreases with increasing  $[\text{H}_2\text{O}_{(\text{g})}]$ . As  $[\text{H}_2\text{O}_{(\text{g})}]$  increases, the generation of OH radicals becomes more efficient and results in higher values for  $\eta_{\text{SO}_2}$ . The more efficient production of OH results primarily from direct electron impact on  $\text{H}_2\text{O}_{(\text{g})}$ , and H abstraction by  $\text{O}(^1D)$  from  $\text{H}_2\text{O}_{(\text{g})}$ . On the other hand, the gas density  $N$  increases as gas temperature decreases. An increase in  $N$  results in a lower reduced electric field ( $E/N$ ) at a constant applied voltage. In addition,  $\text{H}_2\text{O}_{(\text{g})}$  is an electronegative gas which increases the rate of electron attachment, resulting in an increase in the minimum  $E/N$ ,  $(E/N)_0$ , required to initiate and sustain the plasma.<sup>(30)</sup> As  $(E/N)_0$  increases, the fraction of the ac cycle over which the plasma can be sustained decreases. Therefore, the decrease in  $\eta_{\text{SO}_2}$  at 100°C with increasing  $[\text{H}_2\text{O}_{(\text{g})}] > 6\%$  by volume is most likely a result of reduced power deposition to the gas stream. We were unable to operate at voltages greater than 25 kV to optimize  $\eta_{\text{SO}_2}$  due to limitations of the existing power supply.

The dependence of  $\eta_{\text{SO}_2}$  on inlet  $[\text{CO}_2]$  at 23 and 25 kV is shown in Fig. 3. The gas streams contained the specified amount of  $\text{CO}_2$ , 1000 ppmv  $\text{SO}_2$ , 6% by volume  $\text{H}_2\text{O}_{(\text{g})}$ , 6% by volume  $\text{O}_2$ , and  $\text{N}_2$  as the carrier gas. The temperature was 130°C.  $\eta_{\text{SO}_2}$  decreases with increasing  $[\text{CO}_2]$  up to 12% by volume. The lower values of  $\eta_{\text{SO}_2}$  at higher values of  $[\text{CO}_2]$  are attributed to the electronegative nature of  $\text{CO}_2$  which acts to increase

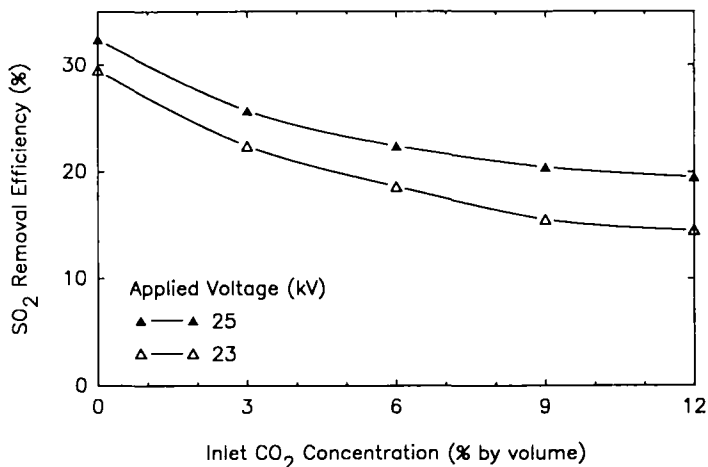


**Fig. 3.** Dependence of  $\eta_{\text{SO}_2}$  on inlet  $[\text{CO}_2]$  and applied voltage. Gas streams are at 130°C with  $\text{SO}_2/\text{O}_2/\text{H}_2\text{O}_{(\text{g})} = 0.1\%/6\%/6\%$  by volume, and  $\text{N}_2$  as the carrier gas. Decreasing values for  $\eta_{\text{SO}_2}$  are likely caused by the electronegative nature of  $\text{CO}_2$  which decreases power deposition to the gas stream.



$(E/N)_0$  and hence decreases the power deposited into the gas stream by the plasma. CO<sub>2</sub> can also intercept a significant fraction of the discharge power, producing CO. The resulting CO rapidly reacts with OH, forming H and CO<sub>2</sub>. Such reaction reduces the [OH], leaving less OH to chemically react with SO<sub>2</sub>.

The rate coefficient for reactions of CO with OH is about  $2 \times 10^{-13} \text{ cm}^3 \text{ s}^{-1}$ . If only 1% of the CO<sub>2</sub> that exists at 12% by volume is converted to CO, then the mean reaction time of OH with CO is about 0.2 ms, which is commensurate with the reaction time of OH with a few ppmv of SO<sub>2</sub>.

The dependence of  $\eta_{\text{SO}_2}$  on inlet [SO<sub>2</sub>] ranging from 250 to 1000 ppmv is shown in Fig. 4 for select processing voltages. Although  $\eta_{\text{SO}_2}$  is higher at a lower inlet [SO<sub>2</sub>], the amount of SO<sub>2</sub> molecules removed from the gas stream is larger for increasing inlet [SO<sub>2</sub>]. Therefore, at a constant gas flow rate and power deposited into the gas stream, the rate of SO<sub>2</sub> molecules removed per unit of time also increases with increasing inlet [SO<sub>2</sub>]. Note that the absolute removal of SO<sub>2</sub> is a function of specific energy deposited to the gas. Higher total removal can be achieved by operating at higher frequencies. This observation indicates that the reactions are possibly kinetically limited due to the relatively short lifetime of OH radicals reacting with species other than SO<sub>2</sub>. This results in a lower absolute removal of SO<sub>2</sub> at a lower inlet [SO<sub>2</sub>].<sup>(26)</sup>

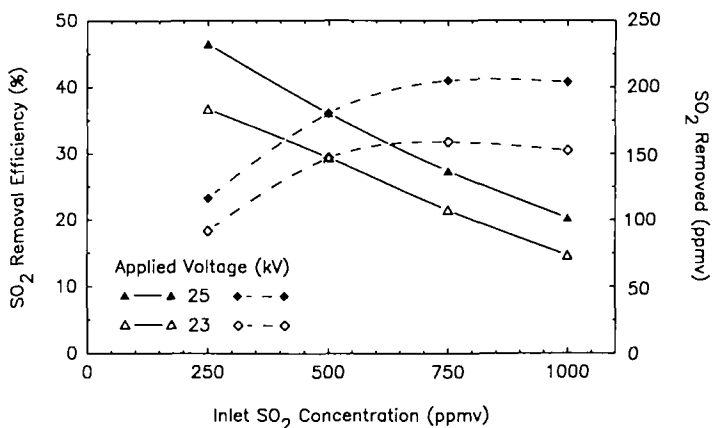


**Fig. 4.** Percent (solid line) and absolute (dashed line) removal of SO<sub>2</sub> as a function of inlet [SO<sub>2</sub>] and voltage at 130°C for gas streams with O<sub>2</sub>/H<sub>2</sub>O(g)/CO<sub>2</sub> = 6%/6%/12% by volume and N<sub>2</sub> as the carrier gas, at a constant power deposition and increasing inlet concentration of SO<sub>2</sub>. The absolute removal of SO<sub>2</sub> increases, while the percent SO<sub>2</sub> removal decreases with increasing inlet [SO<sub>2</sub>].

Removal of  $\text{SO}_2$  is, to a first order, limited by the rate of generation of OH radicals. If  $\text{H}_2\text{O}_{(\text{g})}$  is not depleted, then the rate of OH generation increases with increasing power deposition, which in turn increases with increasing repetition rate. Since the products of  $\text{SO}_2$  removal constitute a small mole fraction, the increase in power deposition should not deplete them by, for example, electron impact dissociation.

Removal of  $\text{SO}_2$  ultimately depends on the number of OH radicals produced, which in turn depends to a first order, on power deposition. As  $[\text{SO}_2]$  increases, this finite supply of OH radicals is used more efficiently. The maximum  $\text{SO}_2$  removal will be achieved when  $[\text{SO}_2]$  is high enough that all OH is consumed by reaction with  $\text{SO}_2$ . At this point, the absolute value of  $\text{SO}_2$  removal can only be increased by a higher rate of generation of OH.

The effect of  $\text{NH}_3$  on  $\eta_{\text{SO}_2}$  was also evaluated at  $130^\circ\text{C}$  (Fig. 5).  $\text{NH}_3$  was injected downstream of the reactor to chemically neutralize  $\text{H}_2\text{SO}_4$  in the gas stream. The amount of back mixing of  $\text{NH}_3$  into the plasma was nominal. The inlet gas stream consisted of the specified amount of  $\text{NH}_3$ ,  $\text{SO}_2/\text{O}_2/\text{CO}_2/\text{H}_2\text{O}_{(\text{g})} = 0.1\%/6\%/12\%/6\%$  by volume, and  $\text{N}_2$  as the carrier gas. The amount of  $\text{NH}_3$  injected into the gas stream is expressed as the stoichiometric ratio (SR) which is defined below:

$$\text{SR} = \frac{[\text{NH}_3]}{2[\text{SO}_2] + [\text{NO}]} \quad (14)$$

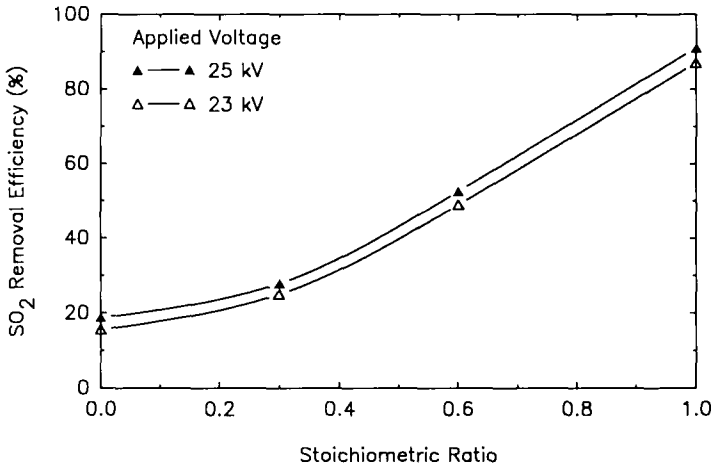
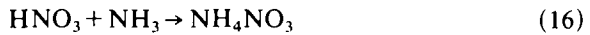


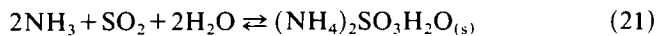
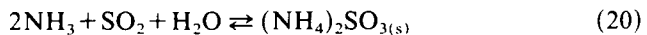
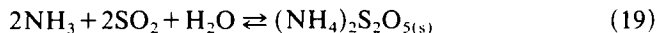
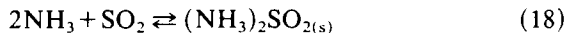
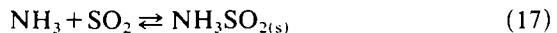
**Fig. 5.**  $\eta_{\text{SO}_2}$  as a function of stoichiometric ratio at  $130^\circ\text{C}$  for gas streams containing  $\text{SO}_2/\text{O}_2/\text{H}_2\text{O}_{(\text{g})}/\text{CO}_2 = 0.1\%/6\%/6\%/12\%$  by volume, and  $\text{N}_2$  as the carrier gas. Increasing values for  $\eta_{\text{SO}_2}$  with increasing stoichiometric ratio are likely caused by thermal reactions between  $\text{SO}_2$  and  $\text{NH}_3$ .

SR is defined as the ratio of actual moles of NH<sub>3</sub> injected into the gas stream divided by the number of stoichiometric moles of NH<sub>3</sub> needed to chemically neutralize the H<sub>2</sub>SO<sub>4</sub> [Eq. (15)] and HNO<sub>3</sub> [Eq. (16)] that would exist in the gas stream if all of the SO<sub>2</sub> is oxidized to H<sub>2</sub>SO<sub>4</sub> and all of the NO is oxidized to HNO<sub>3</sub>.



$\eta_{\text{SO}_2}$  increases from 20 to 90% as SR increases from 0 to 1. To clarify the effects of NH<sub>3</sub> injection and DBDs on  $\eta_{\text{SO}_2}$ , NH<sub>3</sub> was also injected upstream of the reactor and injected without the generation of the DBDs. Experimental results obtained all agree well (within 5%) with that reported in Fig. 5, and white solid particles were observed to deposit on the inner wall of the reactor and tubing during all three cases. These observations indicate that SO<sub>2</sub> removal was mostly attributed to thermal reactions between SO<sub>2</sub>, NH<sub>3</sub>, and H<sub>2</sub>O<sub>(g)</sub> rather than simple chemical neutralization of H<sub>2</sub>SO<sub>4</sub> by NH<sub>3</sub> or other plasma reactions between NH<sub>3</sub> and gas-phase radicals.

The thermal reactions between SO<sub>2</sub>, NH<sub>3</sub>, and H<sub>2</sub>O<sub>(g)</sub> have been studied by other researchers,<sup>(32-36)</sup> and in fact NH<sub>3</sub> injection has been proposed as a method to remove SO<sub>2</sub> from flue gas streams.<sup>(37)</sup> The thermal reactions responsible for SO<sub>2</sub> removal are believed to include at least the following six reactions<sup>(33)</sup>:



Although the precise rate coefficients for these processes are not known, experimental results<sup>(33)</sup> place a lower limit on the effective rate coefficient for SO<sub>2</sub> removal by NH<sub>3</sub> of 10<sup>-16</sup> cm<sup>3</sup> s<sup>-1</sup>.

The use of DBDs to simultaneously remove SO<sub>2</sub> and NO from gas streams was evaluated at 100, 130 and 160°C, respectively (Fig. 6). Inlet

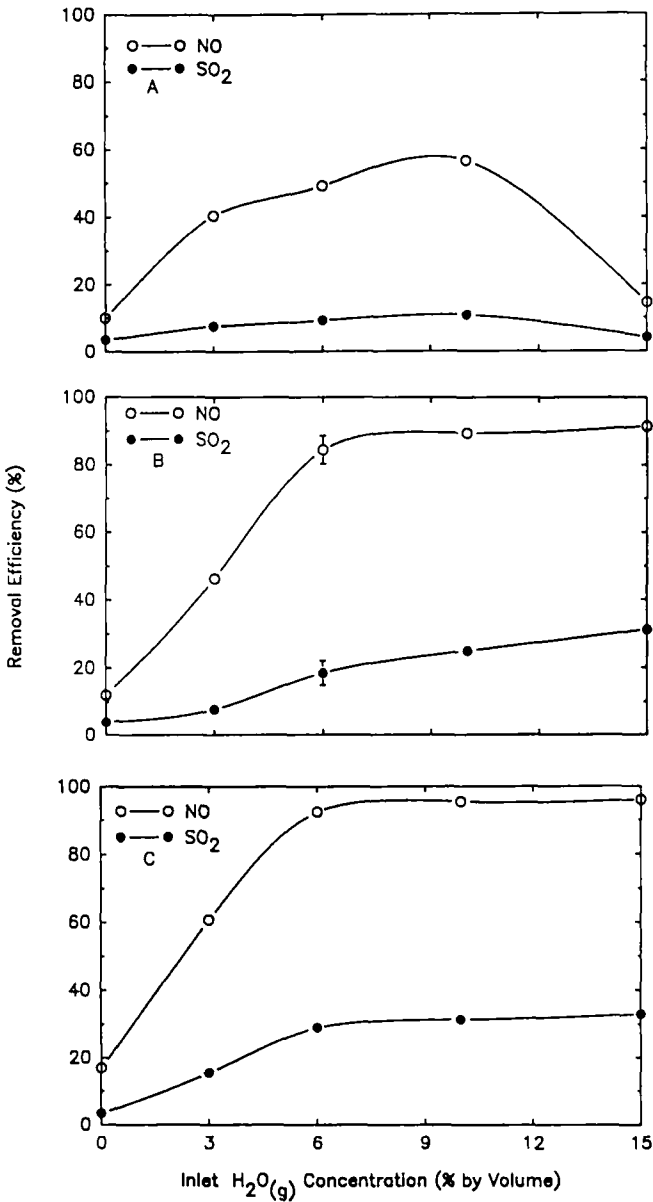


Fig. 6. Dependence of  $\eta_{SO_2}$  and  $\eta_{NO}$  on inlet  $[H_2O(g)]$  at 100°C (A), 130°C (B), and 160°C (C) for gas streams containing  $SO_2/NO/O_2/CO_2 = 0.1\%/0.25\%/6\%/12\%$  by volume, and  $N_2$  as the carrier gas. The applied voltage is 25 kV.

[SO<sub>2</sub>] and [NO] in the gas streams were 1000 and 250 ppmv, respectively. Error bars for  $\eta_{\text{SO}_2}$  and  $\eta_{\text{NO}}$  represent the standard deviations of the test results obtained from four separate sets of measurements. Other results describing the experimental errors have been reported.<sup>(30)</sup>  $\eta_{\text{SO}_2}$  and  $\eta_{\text{NO}}$  increase with increasing temperature, in part, as a result of the increase in  $E/N$ . At 130 and 160°C,  $\eta_{\text{SO}_2}$  and  $\eta_{\text{NO}}$  also increase with increasing [H<sub>2</sub>O<sub>(g)</sub>] due to more efficient generation of OH radicals. At 160°C, with 15% by volume H<sub>2</sub>O<sub>(g)</sub> in the gas stream, more than 95% of the NO and 32% of the SO<sub>2</sub> are simultaneously removed from the gas stream. However, reduced values for  $\eta_{\text{SO}_2}$  and  $\eta_{\text{NO}}$  were obtained at 100°C with 15% by volume H<sub>2</sub>O<sub>(g)</sub>, primarily due to lower power deposition to the gas stream.

Removal of NO<sub>x</sub>, which includes NO and NO<sub>2</sub>, was also investigated. With O<sub>2</sub> in the gas stream, a portion of NO is oxidized to form NO<sub>2</sub> and is detected as NO<sub>x</sub>. Such oxidation results in [NO<sub>x</sub>] being about 30 ppmv higher than [NO]. In all tests,  $\eta_{\text{NO}_x}$  closely followed the same trends as  $\eta_{\text{NO}}$  except  $\eta_{\text{NO}_x}$  was about 10% to 15% lower than  $\eta_{\text{NO}}$  (e.g., 80% for  $\eta_{\text{NO}}$  compared to 65–70% for  $\eta_{\text{NO}_x}$ ). Lower values for  $\eta_{\text{NO}_x}$  compared with  $\eta_{\text{NO}}$  are attributed to the slightly higher inlet [NO<sub>x</sub>], the possible oxidation of NO to NO<sub>2</sub> instead of to HNO<sub>3</sub>, and the possible existence of other oxides of nitrogen that are detectable by chemiluminescence.

The value of  $\eta_{\text{SO}_2}$  is lower than that of  $\eta_{\text{NO}}$ , under the same operating conditions, due to the higher inlet [SO<sub>2</sub>] and lower reaction rate constants for SO<sub>2</sub> and gas-phase radicals as previously described.  $\eta_{\text{SO}_2}$  can be increased by operating the DBD reactor at higher power deposition. Nevertheless, simultaneous removal of SO<sub>2</sub> and NO from gas streams can be achieved with DBDs.

The dependence of the simultaneous removal of SO<sub>2</sub> and NO on NH<sub>3</sub> injection was also evaluated (Fig. 7). As SR increases from 0 to 1,  $\eta_{\text{SO}_2}$  increases from 10 to 100% while  $\eta_{\text{NO}}$  remains nearly constant.  $\eta_{\text{SO}_2}$  is higher during these tests compared with tests removing SO<sub>2</sub> only with NH<sub>3</sub> injection because NH<sub>3</sub> that was to react with NO actually reacted with SO<sub>2</sub>. Injection of NH<sub>3</sub> did not appear to affect  $\eta_{\text{NO}}$  at these relatively low temperatures because NH<sub>3</sub> is unreactive with NO over time scales of 1–10 sec. Increased  $\eta_{\text{SO}_2}$  with NH<sub>3</sub> injection is attributed to the previously mentioned thermal reactions between NH<sub>3</sub> and SO<sub>2</sub> instead of chemical reactions associated with the DBD plasma.

Accurate measurement of the power deposited into the gas stream<sup>(38)</sup> is difficult with the power supply used to generate the DBDs,<sup>(30)</sup> although results from experimental and numerical modeling estimate that tens of millijoules per milliliter of gas is required to remove 90% of the NO from a gas stream initially containing 250 ppmv of NO.<sup>(26)</sup>

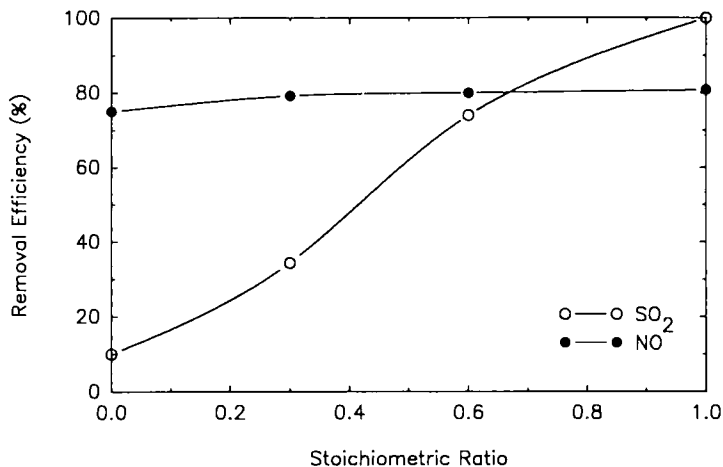


Fig. 7.  $\eta_{\text{SO}_2}$  and  $\eta_{\text{NO}}$  as a function of stoichiometric ratio at 130°C for gas streams containing  $\text{SO}_2/\text{NO}/\text{O}_2/\text{H}_2\text{O}_{(\text{g})}/\text{CO}_2 = 0.1\%/0.025\%/5\%/6\%/12\%$  by volume, and  $\text{N}_2$  as the carrier gas. The applied voltage is 25 kV. Increasing values for  $\eta_{\text{SO}_2}$  with increasing stoichiometric ratio are likely caused by thermal reactions between  $\text{SO}_2$  and  $\text{NH}_3$ .

## 6. SUMMARY AND CONCLUSIONS

The effectiveness of using dielectric barrier discharges to remove  $\text{SO}_2$  and to simultaneously remove  $\text{SO}_2$  and  $\text{NO}$  from gas streams was evaluated experimentally with a laboratory-scale reactor. Removal efficiencies of  $\text{SO}_2$  and  $\text{NO}$  are dependent on applied voltage, inlet concentrations of  $\text{SO}_2$ ,  $\text{NO}$ , and  $\text{H}_2\text{O}_{(\text{g})}$ , and temperature of the gas stream. Simultaneous removal efficiencies for  $\text{SO}_2$  and  $\text{NO}$  at inlet concentrations of 1000 and 250 ppmv are as high as 32 and 95%, respectively. Higher temperatures result in higher removal efficiencies for a given applied voltage due to higher reduced electric field values.  $\text{NH}_3$  injection enhances  $\text{SO}_2$  removal to 100% most likely by thermal reactions between  $\text{SO}_2$  and  $\text{NH}_3$ . These results indicate that DBD plasmas have the potential to simultaneously remove  $\text{SO}_2$  and  $\text{NO}$  from gas streams generated by large-scale fossil fuel combustors.

## ACKNOWLEDGMENTS

The authors acknowledge funding from the U.S. Environmental Protection Agency under Cooperative Agreement CR 812582 to the Advanced Environmental Control Technology Research Center, University of Illinois at Urbana-Champaign, Urbana, Illinois, the National Science Foundation (CTS 88-03170 and ECS 88-15871), and Los Alamos National Laboratory. Although this research has been funded in part by the United States

Environmental Protection Agency, it has not been subjected to the Agency's required peer and administrative review. It therefore does not necessarily reflect the views of the Agency and no official endorsement should be inferred.

## REFERENCES

1. J. D. Spengler, M. Brauer, and P. Koutrakis, *Environ. Sci. Technol.* **24**, 946 (1990).
2. P. J. Temple, *J. Air Pollut. Control Assoc.* **22**, 271 (1972).
3. E. O. Edney, D. C. Stiles, and J. W. Spence, A Laboratory Study to Evaluate the Impact of NO<sub>x</sub> and Oxidants on Atmospheric Corrosion of Galvanized Steel, *ACS Symp. Ser.* **318**, 172 (1986).
4. E. B. Cowling, *Environ. Sci. Technol.* **16**, 110A (1982).
5. M. E. Bassett and J. H. Seinfeld, *Atmos. Environ.* **18**, 1163 (1984).
6. C. S. Sloane and G. T. Wolff, *Atmos. Environ.* **19**, 669 (1985).
7. H. B. Singh, *Environ. Sci. Technol.* **21**, 320 (1987).
8. C. V. Mathai, *J. Air Waste Manage. Assoc.* **40**, 1486 (1990).
9. L. M. Thomas, *USEPA J.* (Oct. 1987).
10. S. Jordan, *Radiat. Phys. Chem.* **31**, 21 (1988).
11. S. Machi, O. Tokunaga, K. Nishimura, S. Hashimoto, W. Kawakami, and M. Washino, *Radiat. Phys. Chem.* **9**, 371 (1977).
12. O. Tokunaga, K. Nishimura, and M. Washino, *International Journal of Applied Radiation and Isotopes* **29**, 87 (1978).
13. N. Frank, S. Hirano, and K. Kawamura, *Radiat. Phys. Chem.* **31**, 57 (1988).
14. H. R. Paur, S. Jordan, and W. Baumann, *J. Aerosol Sci.* **19**, 1397-1400 (1988).
15. B. Eliasson and B. Gellert, *J. Appl. Phys.* **68**, 2026 (1990).
16. J. G. Calvert and W. R. Stockwell, *Mechanism and Rates of the Gas-Phase Oxidations of Sulfur Dioxide and Nitrogen Oxides in the Atmosphere*, Ann Arbor Scientific Publication, Ann Arbor (1984).
17. F. Yin, D. Grosjean, and J. H. Seinfeld, *J. Geophys. Res.* **91**, 14417 (1986).
18. J. D. Butler, *Air Pollution Chemistry*, Academic Press, New York (1979), p. 275.
19. D. L. Baulch, R. A. Cox, and P. J. Crutzen, *J. Phys. Chem. Ref. Data* **11**, 327 (1982).
20. O. Tokunaga and N. Suzuki, *Radiat. Phys. Chem.* **24**, 145 (1984).
21. C. Willis and A. D. Boyd, *Int. J. Radiat. Phys. Chem.* **8**, 71 (1976).
22. U. Kogelschatz, B. Eliasson, and M. Hirth, *Ozone Sci. Technol.* **10**, 367 (1988).
23. B. Eliasson, M. Hirth, and U. Kogelschatz, *J. Phys. D: Appl. Phys.* **20**, 1421 (1987).
24. W. R. Browne and E. E. Stone, Sulfur Dioxide Conversion under Corona Discharge Catalysis, prepared for HEW under contract PH 86-65-2 (1965).
25. I. Sardja and S. K. Dhali, *Appl. Phys. Lett.* **56**, 21 (1990).
26. M. B. Chang, J. H. Balbach, M. J. Rood, and M. J. Kushner, *J. Appl. Phys.* **69**, 4409 (1991).
27. W. C. Neely, E. I. Newhouse, and S. Pathirana, *Chem. Phys. Lett.* **155**, 381 (1989).
28. J. W. Bozzelli and R. B. Barat, *Plasma Chem. Plasma Process.* **8**, 293 (1988).
29. G. H. Ramsey, N. Plaks, W. H. Ponder, B. E. Daniel, and L. E. Hamel, Proceedings of the 83rd Annual Air and Waste Management Association Meeting, Pittsburgh, Pennsylvania, Paper No. 90-109.2 (1990).
30. M. B. Chang, M. J. Kushner, and M. J. Rood, *Environ. Sci. Technol.* **26**, 777-781 (1992).
31. A. M. Winer, J. W. Peters, J. P. Smith, and J. N. Pitts, Jr., *Atmos. Environ.* **18**, 5 (1984).
32. J. C. Person and D. O. Ham, *Radiat. Phys. Chem.* **31**, 1 (1988).

33. H. Bai, P. Biswas, and T. C. Keener, Proceedings of the 84th Annual Air and Waste Management Association Meeting, Vancouver, B.C., Canada, Paper No. 91-103.24 (1991).
34. R. Landreth, R. G. de Pena, and J. Heicklen, *J. Phys. Chem.* **89**, 9 (1985).
35. R. W. Tock, K. C. Hoover, and G. J. Faust, SO<sub>2</sub> Removal by Transformation to Solid Crystals of NH<sub>3</sub> Complexes, *AIChE Symp. Ser.* **188**, 75 (1979).
36. T. C. Keener and W. T. Davis, Demonstration of a Ca(OH)<sub>2</sub>/NH<sub>3</sub> Based System for the Removal of SO<sub>2</sub> on High Sulfur Coals, Ohio Coal Development Office, Columbus, Ohio, August, 1988.
37. C. C. Shale, Ammonia Injection: A Route to Clean Stacks, *Pollution Control and Energy Needs*, R. M. Jameson and R. S. Spindt, eds., Advances in Chemistry Series, **127**, 195-205 (1973).
38. J. J. Carlins, *Environ. Prog.* **1**, 2, 113-118 (1982).